Inelastic longitudinal electron scattering C2 form factors in ^{58}Ni

Firas Z. Majeed, Fadhel M. Hmood

Department of Physics, College of Science, Baghdad University, Baghdad, Iraq

E-mail: abosajjad_altamemme@yahoo.com

Abstract

Inelastic longitudinal electron scattering form factors for the excitation of 2^+ in ^{58}Ni nucleus have been studied through nuclear shell model of the ($p_{3/2}$,$p_{1/2}$,$1f_{5/2}$) configurations. Effective transition operators relevant to the model space are derived by considering particle-hole excitation from the core orbits and via the model space orbits into the higher orbits with $2\hbar\omega$ for *C2* transition within the framework of a first-order perturbation theory. Using F5PVH potential as an effective interaction to generate the model space wave function. The simple harmonic oscillator (HO) potential is used to generate the single particle wave functions.

Discarded space (core orbits + higher configuration orbits) will be included as a first order correction which is the so called core polarization effect.

Modern realistic interaction of the two body Michigan sum of three range Yukawa potential (M3Y-P2) and Gogny have been adopted as a residual interactions to couple the particle-hole pair.

The investigated nucleus is considered to be consisting of ^{56}Ni core nucleus plus extra valence nucleons represented by two neutrons distributed over fp-shell.

The obtained theoretical results had been compared with available experimental data.

Keywords

Core polarization, ^{58}Ni, form factor.

Article info.

Received: Sep. 2015

Accepted: Nov. 2015

Published: Apr. 2016

عوامل التشكل الطولية للاستطارة الالكترونية غير المرنة C2 لنواة النيكل ^{58}Ni

فراس زهير مجيد، فاضل محمود حمود

قسم الفيزياء ،كلية العلوم، جامعة بغداد، بغداد، العراق

الخلاصة

تم دراسة عوامل التشكل الطولية للاستطارة الالكترونية غير المرنة C2 لنواة النيكل^{58}Ni لحالة التهيج 2^+من خلال نظرية القشرة النووية للتشكيلات ($p_{3/2}$,$p_{1/2}$,$1f_{5/2}$) من خلال انتاج زوج جسيم-فجوة من اوربيتالات القلب الخامل الى اوربيتالات التشكيلات العليا عبر اوربيتالات أنموذج الفضاء بطاقة تهيج مقدارها $2\hbar\omega$ للانتقال C2 من خلال نظرية الاضطراب من المرتبة الاولى، وباستخدام جهد التفاعل F5PVHكتفاعل فعال لنموذج الفضاء.تم استخدام جهد المتذبذب التوافقي البسيط لتوليد دالة الموجة للجسيم المنفرد.

الفضاء المستثنى المتضمن اوربيتالات القلب واوربيتالات التشكيلات العليا تم تضمينها كتصحيح من المرتبة الاولى والذي يدعى تاثير استقطاب القلب.تم استخدام التفاعلين M3Y-P2 وGogny كتفاعل بقية لربط الزوج جسيم- فجوة.

اعتبرت النواة انها تتالف من النواة ^{56}Ni كنواة قلب مع توزيع النيكولونات الاضافية المتمثلة بزوج من النيوترونات على اغلفة انموذج الفضاء وقد قورنت النتائج النظرية مع البيانات التجريبية المتوفرة.

Introduction

The electron scattering from the nucleus at high energy gives perfect and good information about the nuclear structure. When the energy of the incident electron is in the range of 100 MeV and more, the de Broglie wavelength will be in the range of the spatial extension of the target nucleus, Thus with these energies, the electron represents a best probe to study the nuclear structure [1,2].

The electrons scattering from a target nucleus can occur in two types: first, the nucleus is left in its ground state after the scattering and the energy of the electrons is unchanged, this processes is called "Elastic Electron Scattering". In the second the scattered electron leaves the nucleus in different excited state which has a final energy reduced from the initial just by the amount taken up by the nucleus in its excited state, this processes is called " Inelastic Electron Scattering" [3,4].

It is known that the inelastic electron scattering has proven to be a good technique for studying the properties of excited states of nuclei, in particular their spins, parities, and the strength and structure of the transition operators connecting the ground and the excited states[5].

Electron scattering is an excellent tool for studying the nuclear structure because of many reasons. Since the interaction between the electron and the target nucleus is relatively weak of order α =1/137, the fine-structure constant, and known where the electron interacts electromagnetically with the local charge, current and magnetization densities of nucleus. [6].

The form factor can be found experimentally as a function of the momentum transfer (q) by knowing the energies of the incident and scattered electron and the scattering angle. The electron scattering process can be explained according to the first Born approximation as an exchange of a virtual photon carrying a momentum between the electron and nucleus. The first Born approximation is being valid only if $Z\alpha<<1$, where α is the fine structure constant [7].

The scattering cross section for relativistic electrons from spinless nucleus of charge Ze, where Z is the number of protons in the nucleus, was first derived by Mott (1929) [8].

The nickel isotopes had been described in terms of strongly admixed spherical shell-model configurations of neutrons occupying the $2p_{3/2}$, $1f_{5/2}$, and $2p_{1/2}$orbits. A set of effective-interaction matrix elements is deduced which accurately reproduces the spectra of the Ni isotopes from Ni^{58} to Ni^{67}. The wave functions resulting from the calculations of the energy levels are then used to calculate the single-nucleon spectroscopic factors. These are in fairly good agreement with the experimental spectroscopic factors found in pickup and stripping experiments. The *E2* transition probabilities in the even-mass isotopes of Ni are calculated and found to be in agreement with experimental facts [9].

A report of experimental for a set of inelastic form-factor measurements on the first excited state of ^{58}Ni, ^{60}Ni, and ^{62}Ni, which, together with the accurate Coulomb-excitation *B(E2)* measurements by Stelson and McGowan, provide for the first time an accurate experimental check on the distorted-wave calculation of Griffy et al. The experimental measurements were carried out at the Yale Linear Electron Accelerator Laboratory using incident energies ranging from 45 to 65 MeV and scattering angles from 70° to 130° [10].

Using the experiment to study the inelastic scattering of electrons from ^{60}Ni with an over-all energy resolution of 0.1% by the use of 183 MeV and

250 MeV electron beams from the Tohoku 300 MeV linear accelerator[11].

Inelastic electron scattering cross sections have been measured up to a momentum transfer q=3.9 fm^{-1}, determining very precisely the transition charge density of the first excited (2^+_1) state of ^{58}Ni. The results have been interpreted in a fully self-consistent theoretical treatment for both the ground state and the (2^+_1) transition charge density of ^{58}Ni [12].

Elastic and inelastic electron-scattering form factors for multipolarities up to L=7 and some transition-strength distributions are calculated with shell-model wave functions for about ten target nuclei in the mass range A = 52-62 including ^{52,53}Cr, ^{54,56}Fe, ^{53}Cr, ^{55}Mn, ^{59}Co and ^{58,60,62}Ni. It is found that the strengths of the calculated magnetic transitions are always less than about 50% of the pure single-particle values [13].

A microscopic description of data on the inelastic scattering for factors for the $0^{+} \rightarrow 2^{+}$ as well as $0^{+} \rightarrow 4^{+}$ transitions in some doubly even Ti, Cr, Fe, Zn, and Ni isotopes including ^{58,60,62}Ni is attempted in terms of the projected Hartree-Fock-Bogoliubov wave functions resulting from realistic effective interactions operating in the *2p-1f* shell [14].

The effective interaction GXPF1 for shell-model calculations in the full pf shell had been tested in detail from various viewpoints such as binding energies, electromagnetic moments and transitions, and excitation spectra. The semi magic structure is successfully described for N or Z=28 nuclei, ^{53}Mn, ^{54}Fe, ^{55}Co, and ^{56,57,58,59}Ni, suggesting the existence of significant core excitations in low-lying model over conventional calculations in cases where full-space calculations still remain too large to be practical [15].

The experimental single-particle energies and occupation probabilities for neutron states near the Fermi energy in ^{58,60,62,64} Ni nuclei had studied and obtained from joint evaluation of the data on nucleon stripping and pickup reactions on the same nucleus. The resulting data had been analyzed within a mean-field model with dispersive optical-model potential. Good agreement had been obtained between the calculated and experimental [16].

High-precision reduced electric-quadrupole transition probabilities B(E2; $0^+_1 \rightarrow 2^+_1$) have been measured from single-step Coulomb excitation of semi-magic ^{58,60,62,64}Ni (Z = 28) beams at 1.8 MeV per nucleon on a natural carbon target. The energy loss of the nickel beams through the carbon target were directly measured with a zero-degree Bragg detector and the absolute $B(E2)$ values were normalized by Rutherford scattering. The $B(E2)$ values disagree with recent lifetime studies that employed the Doppler-shift attenuation method [17].

Calculated elastic and inelastic form factors and for the transition from the ground state to $J^+_{\|}$ (L = J = 2, 4) state in $^{58-68}$Ni and ^{24}Mg, carried out the starting point of method was a set of Hartree-Fock-Bogoliubov wave functions generated with a constraint on the axial quadrupole moment and using a Skyrme energy density functional [18].

The Core Polarization (CP) effects derivation with higher configuration in the first order perturbation theory and the two-body matrix elements of three parts of realistic interaction: central, spin orbit and tensor force which are belong to M3Y-P2 and Gogny as a residual interactions in a separate pictures will be studied in the present work.

A computer program is written in FORTRAN 90 language to include realistic interaction M3Y and Gogny in the original code which is written by [19].

Theory

Many particle matrix elements of the electron scattering operator $\hat{T}^{\eta}_{\Lambda}$ are expressed as the sum of the product of the one-body density matrix elements (OBDM) times the single-particle transition matrix elements [20]:

$$\left\langle \Gamma_f \left\| \hat{T}^{\eta}_{\Lambda} \right\| \Gamma_i \right\rangle = \sum_{\alpha,\beta} OBDM\left(\Gamma_i,\Gamma_f,\alpha,\beta\right)\left\langle \alpha \left\| \hat{T}^{\eta}_{\Lambda} \right\| \beta \right\rangle \quad (1)$$

where $\Lambda = JT$ is the multipolarity in spin and isospin respectively, and the states $\Gamma_i \equiv J_i T_i$ and $\Gamma_f \equiv J_f T_f$ are the initial and final states of the nucleus, while α and β denote the final and initial single-particle states, respectively (isospin is included), the superscript η represents longitudinal (L) or transverse (T) (electric(El) or magnetic (mag)). The reduced matrix elements of the electron scattering operator $\hat{T}^{\eta}_{\Lambda}$ consist of two parts, one is the "Model space" matrix elements and the other is the "Core-polarization" matrix elements [21].

$$\left\langle \Gamma_f \left\| \hat{T}^{\eta}_{\Lambda} \right\| \Gamma_i \right\rangle = \left\langle \Gamma_f \left\| \hat{T}^{\eta}_{\Lambda} \right\| \Gamma_i \right\rangle_{MS} + \left\langle \Gamma_f \left\| \delta\hat{T}^{\eta}_{\Lambda} \right\| \Gamma_i \right\rangle_{CP} \quad (2)$$

$\left\langle \Gamma_f \left\| \hat{T}^{\eta}_{\Lambda} \right\| \Gamma_i \right\rangle_{MS}$ is the model-space matrix elements.

$\left\langle \Gamma_f \left\| \delta\hat{T}^{\eta}_{\Lambda} \right\| \Gamma_i \right\rangle_{CP}$ is the core-polarization matrix elements.

$\left|\Gamma_i\right\rangle$ and $\left|\Gamma_f\right\rangle$ are described by the model-space wave functions.

The model-space matrix elements are expressed as the sum of the product of the one-body density matrix elements (OBDM) times the single-particle matrix elements which are given by:

$$\left\langle \Gamma_f \left\| \hat{T}^{\eta}_{\Lambda} \right\| \Gamma_i \right\rangle_{MS} = \sum_{\alpha,\beta} OBDM\left(\Gamma_i,\Gamma_f,\alpha,\beta\right)\left\langle \alpha \left\| \hat{T}^{\eta}_{\Lambda} \right\| \beta \right\rangle_{MS} \quad (3)$$

The core-polarization matrix element in Eq. (2) can be written as follows[21]:

$$\left\langle \Gamma_f \left\| \delta\hat{T}^{\eta}_{\Lambda} \right\| \Gamma_i \right\rangle_{cp} = \sum_{\alpha,\beta} OBDM\left(\Gamma_i,\Gamma_f,\alpha,\beta\right)\left\langle \alpha \left\| \delta\hat{T}^{\eta}_{\Lambda} \right\| \beta \right\rangle_{cp} \quad (4)$$

According to the first order perturbation theory, the single-particle matrix element for the higher-energy configurations is given by [22]:

$$\left\langle \alpha \left| \delta\hat{T}^{\eta}_{J} \right| \beta \right\rangle = \left\langle \alpha \left| \hat{T}^{\eta}_{J} \frac{Q}{E - H^{(0)}} V_{res} \right| \beta \right\rangle + \left\langle \alpha \left| V_{res} \frac{Q}{E - H^{(0)}} \hat{T}^{\eta}_{J} \right| \beta \right\rangle \quad (5)$$

where V_{res} is adopted here as a residual nucleon-nucleon interaction.

The single-particle energies are calculated according to [22]:

$$e_{nlj}=(2n+l-\frac{1}{2})\hbar\omega+\begin{cases}-\frac{1}{2}(l+1)\langle f(r)\rangle_{nl} & for\ j=l-\frac{1}{2}\\ \frac{1}{2}l\langle f(r)\rangle_{nl} & for\ j=l+\frac{1}{2}\end{cases} \quad (6)$$

with:

$$\langle f(r)\rangle_{nl}\approx -20A^{-2/3}MeV \quad (7)$$

$$\hbar\omega=45A^{-1/3}-25A^{-2/3}$$

The realistic M3Y and Gogny effective NN interaction, which is used in electron scattering (V_{res} =v12) is expressed as a sum of the central potential part $v_{12}^{(C)}$, spin-orbit potential part $v_{12}^{(LS)}$, long range tensor part $v_{12}^{(TN)}$, and density dependence part $v_{12}^{(DD)}$ as follows[23]:

$$v_{12}=v_{12}^{(c)}+v_{12}^{(LS)}+v_{12}^{(TN)}+v_{12}^{(DD)} \quad (8)$$

The four potentials are expressed as[23]:

$$\begin{aligned}
v_{12}^{(c)}&=\sum_n(t_n^{(SE)}P_{SE}+t_n^{TE}P_{TE}+t_n^{(SO)}P_{SO}+t_n^{(TO)}P_{TO})f_n^{(C)}(r_{12})\\
v_{12}^{(LS)}&=\sum_n(t_n^{(LSE)}P_{TE}+t_n^{(LSO)}P_{TO})f_n^{(LS)}(r_{12})L_{12}\cdot(\vec{s}_1+\vec{s}_2)\\
v_{12}^{(TN)}&=\sum_n(t_n^{(TNE)}P_{TE}+t_n^{(TNO)}P_{TO})f_n^{(TN)}(r_{12})r_{12}^2S_{12}\\
v_{12}^{(DD)}&=\left\{t^{DD}P_{SE}\cdot[\rho(r_1)]^{a^{(SE)}}+t^{DD}P_{TE}\cdot[\rho(r_1)]^{a^{(TE)}}\right\}\delta(r_{12})
\end{aligned} \quad (9)$$

where $f_n(r)=\frac{e^{-\mu_n r}}{\mu_n r}$ for M3Y interaction, μ_n: range parameter $f_n^{C}(r)=e^{-(\mu_n r)^2}$, $f_n^{LS}=\nabla^2\delta(r)$ represented Gogny interaction, then for M3Y,

Eq. (9) becomes:

$$\begin{aligned}
v_{12}^{(c)}&=\sum_n(t_n^{(SE)}P_{SE}+t_n^{TE}P_{TE}+t_n^{(SO)}P_{SO}+t_n^{(TO)}P_{TO})\frac{e^{-\mu_n r}}{\mu_n r}\\
v_{12}^{(LS)}&=\sum_n(t_n^{(LSE)}P_{TE}+t_n^{(LSO)}P_{TO})f_n^{(LS)}(r_{12})L_{12}\cdot(\vec{s}_1+\vec{s}_2)\\
v_{12}^{(TN)}&=\sum_n(t_n^{(TNE)}P_{TE}+t_n^{(TNO)}P_{TO})f_n^{(TN)}(r_{12})r_{12}^2S_{12}\\
v_{12}^{(DD)}&=\left\{t^{DD}P_{SE}\cdot[\rho(r_1)]^{a^{(SE)}}+t^{DD}P_{TE}\cdot[\rho(r_1)]^{a^{(TE)}}\right\}\delta(r_{12})
\end{aligned} \quad (10)$$

And for Gogny Eq.(9) becomes:

$$\begin{aligned}
v_{12}^{(c)}&=\sum_n(t_n^{(SE)}P_{SE}+t_n^{TE}P_{TE}+t_n^{(SO)}P_{SO}+t_n^{(TO)}P_{TO})e^{-(\mu_n r)^2}\\
v_{12}^{(LS)}&=\sum_n(t_n^{(LSE)}P_{TE}+t_n^{(LSO)}P_{TO})\nabla^2\delta(r)L_{12}\cdot(\vec{s}_1+\vec{s}_2)\\
v_{12}^{(TN)}&=\sum_n(t_n^{(TNE)}P_{TE}+t_n^{(TNO)}P_{TO})f_n^{(TN)}(r_{12})r_{12}^2S_{12}\\
v_{12}^{(DD)}&=\left\{t^{DD}P_{SE}\cdot[\rho(r_1)]^{a^{(SE)}}+t^{DD}P_{TE}\cdot[\rho(r_1)]^{a^{(TE)}}\right\}\delta(r_{12})
\end{aligned} \quad (11)$$

where $t_n^{(SE)}$, $t_n^{(SO)}$, $t_n^{(TO)}$, $t_n^{(TE)}$ are the strength parameter in central part for (singlet-even), (singlet-odd), (triplet-odd) and (triplet-even), and $t_n^{(LSE)}$, $t_n^{(LSO)}$ are the strength parameter in the spin –orbit part for (singlet-even), (singlet-odd), $t_n^{(TNE)}$, $t_n^{(TNO)}$, are the strength parameter in tensor part for (tensor even), (tensor-odd) and $t_{DD}^{(SE)}$, $t_{DD}^{(TE)}$ are the strength parameter in density dependence parts for (single-even), (triplet-even) respectively.

The first range parameters of the interaction (R_1) between two nucleons in centeral and spin-orbit force is 0.25 fm, the second range (R_2) is 0.4 fm, and the longest range (R_3) is 1.414 fm. These parameter values are given in Table 1 [23].

Table 1: The values of the best fit to the potential parameters for M3Y-P2 [23].

	R_1=0.25 fm	R_2=0.40 fm	R_3=1.414 fm
Oscillator matrix elements (Channel)	t_1 MeV	t_2 MeV	t_3 MeV
Centeral Singlet-Even (SE)	8027	-2880	-10.463
Central Triplet-Even (TE)	6080	2730	31.389
Central Singlet-Odd (SO)	-11900	-4266	-10.463
Central Triplet-Odd (TO)	3800	-780	3.488
Tensor-Even(TNE)	-131.52 MeV fm^{-2}	-3.708 MeV fm^{-2}	0.0
Tensor-Odd(TNO)	29.28 MeV fm^{-2}	1.872 MeV fm^{-2}	0.0
Spin-Orbit Even(LSE)	-9181.8	-606.6	0.0
Spin-Orbit Odd(LSO)	-3414.6	0.0	0.0
Density- single even (SE)	181 MeV fm	0.0	0.0
Density- Triplet even (TE)	1139 MeV fm	0.0	0.0

Results and discussion

The model space adopted in this work is $2p_{3/2}$ $1f_{5/2}$ $2p_{1/2}$ configuration for ^{58}Ni nucleus. Core-polarization effects are taken into account through first order perturbation theory, which allows particle-hole excitation from shell core orbits $1s_{1/2}$, $1p_{3/2}$, $1p_{1/2}$, $1d_{5/2}$, $2S_{1/2}$, $1d_{3/2}$ and $1f_{7/2}$ (shell model space having ^{56}Ni as an inert core).

The model space effective interaction F5PVH potential has been used to give the ($1f_{5/2}2p_{3/2}2p_{1/2}$) shell model wave functions for ^{58}Ni.

The single particle wave functions of the harmonic oscillator (HO) with size parameter b= 1.988 fm are used [24].

The longitudinal C2 form factors of ^{58}Ni from the ground state ($J^{\pi}T=0^{+}1$) to the excited state ($J^{\pi}T=2^{+}1$) at E_x=1.398 MeV have been calculated with core contribution only, since the model space of neutrons has no contribution to the charge form factor, because they are neutral particles, then only core protons will be taken into account. Two realistic interactions M3Y-P2 and Gogny as a residual interaction are used.

Fig.1 by using M3Y interaction shows that an excellent agreement is obtained for the first maxima (3×10^{-3}) of the form factor for momentum transfer range $0\leq q\leq 1.75 fm^{-1}$, where the data are correctly reproduced up to q=1.4 fm^{-1}, but the second maximum

(1×10^{-5}) for region q~1.75 fm^{-1} to q~3.5 fm^{-1} had been quenched, that is clear, the calculations underestimate the experimental data, there are a clear deviation in diffraction minima from the theoretical calculation to the experimental data approximately 0.5 fm^{-1} with respect to the q values.

Fig.2 using Gogny interaction shows that the form factor value about $3x10^{-3}$ represented the first maximum for the range $0\leq q\leq 1.75 fm^{-1}$, which is an excellent agreement is obtained with experimental data up to q=1.5 fm^{-1}, but the second maximum (6×10^{-6}) for region q~1.75 fm^{-1} to q~3.5 fm^{-1} have been quenched, clearly the calculations underestimate the experimental data.

The OBDM elements for this transition are shown in Table2. The experimental data are taken from Ref. [18].

Table 2: The values of the OBDM elements for the longitudinal C2 transition of the 2^+_1, first state of ^{58}Ni using F5PVH model space effective interaction, with the residual interaction M3Y and Gogny at E_X=1.398 MeV.

J_i	J_f	OBDM ($\Delta T=0$)	OBDM ($\Delta T=1$)
5/2	5/2	-0.13643	-0.11140
5/2	3/2	0.13559	0.11071
5/2	1/2	-0.13677	-0.11167
3/2	5/2	-0.07833	-0.06396
3/2	3/2	-0.65956	-0.53853
3/2	1/2	-0.19730	-0.16110
1/2	5/2	-0.14353	-0.11719
1/2	3/2	0.35839	0.29263

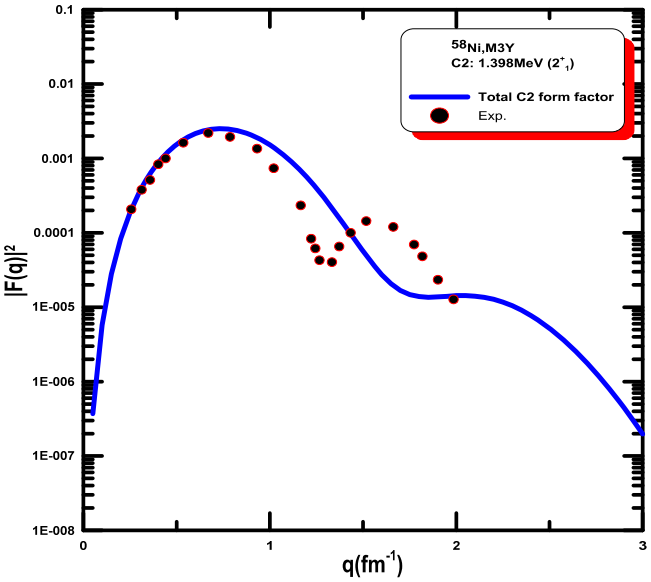

Fig.1: Inelastic longitudinal C2 form factors (total) for the 2^+_1 (E_x=1.398 MeV) state in ^{58}Ni with M3Y, theoretical data represented by solid curve, the experimental data (filled circles) are taken from Ref. [18].

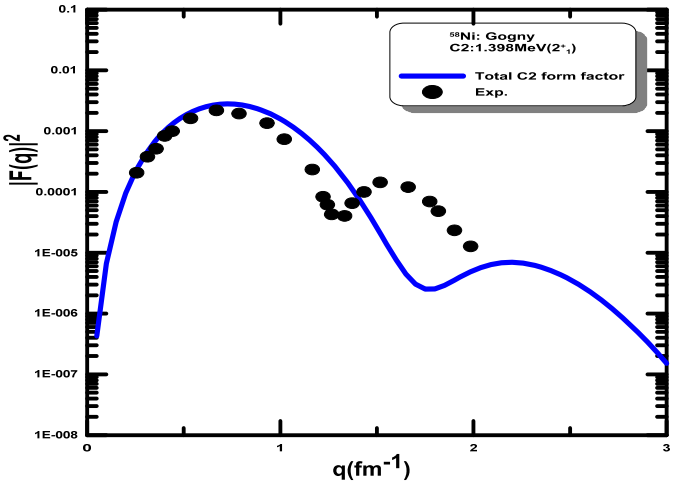

Fig.2: Inelastic longitudinal C2 form factors for the 2_1^+ ***(E_x=1.398 MeV) state in*** ^{58}Ni ***with Gogny, theoretical data represented by solid curve, the experimental data (filled circle) are taken from Ref. [18].***

Fig.3 shows the quadrupole C2 charge form factors for second transition from the ground state ($J^\pi T=0^+1$) to the final state ($J^\pi T=2^+1$) at E_x=2.743 MeV, with a residual interaction M3Y, for the second lobe a good agreement with maxima value of form factor 3×10^{-3} at $0 \le q \le 1.25$ fm^{-1}, one can see that the results are very small almost be neglected, while the second lobe with value of form factor 1×10^{-3} for momentum transfer region from q~1.25 fm^{-1} to q~3.25 fm^{-1}. It is clear that calculations deflected in phase and overestimates, the difference between the calculation and experimental data are about 9 with respect to form factor value.

From Fig. 4, for first maximum the theoretical data overestimate the experimental data and the difference between experimental data and theoretical calculation is very small with respect to form factor values, which is equal to 4×10^{-3} at range from 0 to 1.25 fm^{-1} with respect to the q values, while the second maximum, the theoretical results overestimate, and the difference between the theoretical and experimental is about 3 with respect to form factor values, the form factor value about 5×10^{-4} for q range $1.25 \le q \le 3$ fm^{-1},

The OBDM elements for these transitions are shown in Table 3. The experimental data are taken from Ref.[18].

Table 3: The values of the OBDM elements for the longitudinal C2 transition of the 2^+1***, second*** 2^+ ***state of*** ^{58}***Ni using F5PVH model space effective interaction for M3Y and Gogny at*** E_X***=2.743 MeV.***

J_i	J_f	OBDM (ΔT=0)	OBDM (ΔT=1)
5/2	5/2	-0.10910	-0.08908
5/2	3/2	0.46568	0.38023
5/2	1/2	-0.05029	-0.04107
3/2	5/2	-0.26904	-0.21967
3/2	3/2	0.56880	0.46442
3/2	1/2	-0.12203	-0.09964,
1/2	5/2	-0.05278	-0.04309
1/2	3/2	0.22167	0.18099

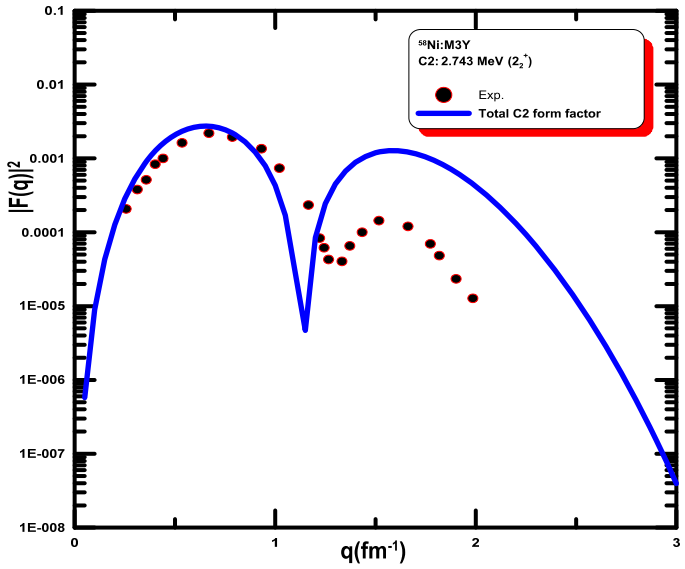

Fig.3: Inelastic longitudinal C2 form factors for the 2_2^+ state (E_X=2.743 MeV) in ^{58}Ni with residual interaction M3Y (solid curve), experimental data (filled circle) are taken from Ref. [18].

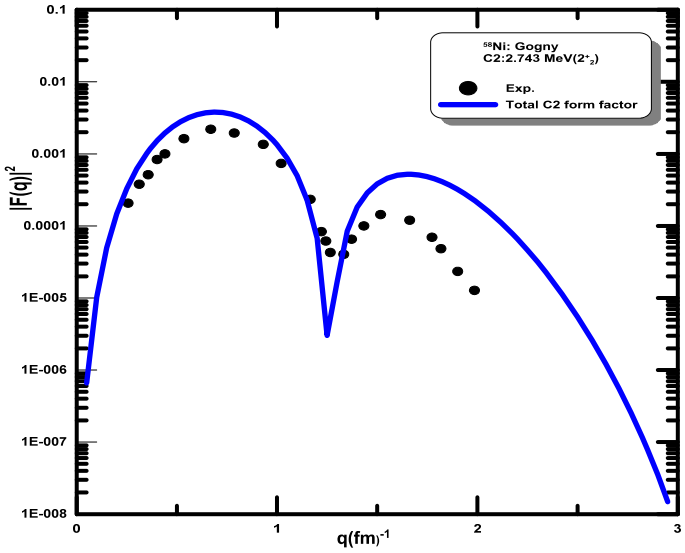

Fig. 4: Inelastic longitudinal C2 form factors for the 2_2^+ state (2.743 MeV) in ^{58}Ni with a residual interaction Gogny (solid curve), experimental data (filled circle) are taken from Ref. [18].

Fig.5 by using M3Y interaction shows the calculation for the C2 transition for third case 2_3^+ from the ground state ($J^\pi T=0^+1$) to the final state ($J^\pi T=2^+1$) at E_x=3.250 MeV, only one lobe obtained from this calculation, the maximum value of form factor about 5×10^{-3} at the momentum transfer region from 0 to 3 fm^{-1}. It is very clear that there is difference between the theoretical and experiment data in shape and magnitude when the results overestimate by 3 with respect to the form factor values.

Fig.6 Gogny shows the calculation for the C2 transition for third case 2_3^+ from the ground state ($J^\pi T=0^+1$) to the final state ($J^\pi T=2^+1$) at E_x=3.250 MeV, only one lobe obtained from this calculation, the maximum value of form factor is about 3×10^{-3} at the momentum transfer region from 0 to 3

fm^{-1}. It is very clear that there is difference between the theoretical and experiment data in shape and magnitude when the results overestimate by 2 with respect to the form factor values.

The OBDM elements for these transitions are shown in Table 4. The experimental data are taken from Ref.[18].

Table 4: The values of the OBDM elements for the longitudinal C2 transition of the 2^+_1, third 2^+ state of 58Ni using F5PVH model space effective interaction., with M3Y and Gogny as a residual interaction at E_X=3.250 MeV.

Ji	Jf	OBDM (ΔT=0)	OBDM (ΔT=1)
5/2	5/2	0.10875	0.08879
5/2	3/2	0.46464	0.37938
5/2	1/2	0.06828	0.05575
3/2	5/2	-0.26844	-0.21918
3/2	3/2	-0.37085	-0.30280
3/2	1/2	0.20316	0.16588
1/2	5/2	0.07166	0.05851
1/2	3/2	-0.36903	-0.30131

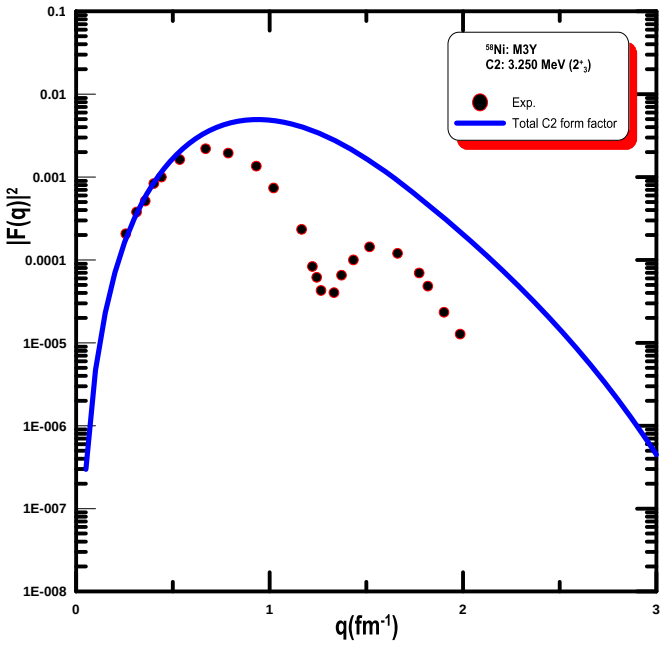

Fig.5: Inelastic longitudinal C2 form factors for the 2^+_3 state at (E_x=3.250 MeV)in ^{58}Ni with M3Y as a residual interaction (solid curve), the experimental data (filled circles) are taken from Ref. [18].

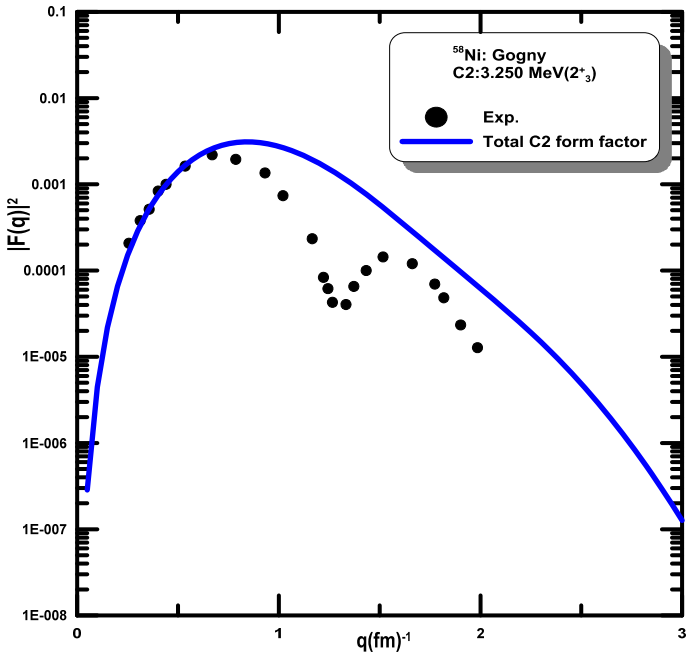

Fig.6: Inelastic longitudinal C2 form factors for the 2^+_3 ***state at Ex= 3.250 MeV in*** ^{58}***Ni with Gognyas a residual interaction (solid curve), experimental data (filled circles) are taken from Ref. [18].***

Conclusions

1. The realistic potential M3Y, and Gogny as a residual interaction used to calculate core –polarization effects has improved the calculation, in general, the results towards the agreement with the experimental data.
2. The core-polarization effect enhances the form factors and makes the theoretical results of the inelastic longitudinal form factors closer to the experimental data in the C2, which is studied in this work.
3. From our calculations for inelastic longitudinal form factor, we founded that for the first inelastic transition represented by C2 that the first transition 2^+_1 with using Gogny is the best one to give us results closer the experimental for all calculation.
4. Present calculations have revealed significant discrepancies vice versa the large-momentum-transfer at (q=1.5 fm^{-1}) for the form factor data.

Acknowledgement

The Authors are very grateful to Prof. Dr. Raad A. Radhi for his assistance to provide the original copy of his two codes of calculation of form factors and residual interaction.

Future research

Choosing of different inert core for the same nucleus will give different results depending on the nucleons in model space whether protons or neutrons, where the presence of protons in the model space gives its role in the calculation, that unless we find it in our calculation as the confinement of protons in the space deprived of contribution for Coulomb transition.

References

[1] R.R.Roy and B.P.Nigam, "Nuclear Physics: Theory and Experiment" Wiley, (1967).

[2]R. Hofstadter, Annual Review of Nuclear Science, 7 (1957) 231.

[3]H.Uberall, "Electron Scattering From Complex Nuclei" Part B, Academic Press, New York, (1971).
[4]B. Ghosh and S. K. Sharma, Phys. Rev. C, 32 (1985) 643.
[5]M. E. Rose, "Polarization of nuclear spins",Technical Information Division, Oak Ridge Operations, (1948) 5.
[6]J. D. Walecka," Electron Scattering for Nuclear and Nucleon Structure" Cambridge University Press, Cambridge, (2001) 14.
[7]N.F.Mott, Proc. Roy. Soci. Ser, A124 (1926) 425.
[8]K. J. M. B. and R. S. Willey, Phys. Rev. Lett. 11(1963) 518.
[9]N. Auerbach, Physical Review, 163, 4 (1967) 1203–1218.
[10]M. A. Duguay, C. K. Bockelman, T. H. Curtis, R. A Eisenstein, Physical Review Letters, 17, 1 (1966) 28.
[11]A. M. K. Y. Torizuka, Y. Kojma, M. Oyamada, K. Sugiyama, T. Terasawa, K. Itoh, A. Yamaguchi, Physical Review, 185 (1969) 4.
[12]B. Frois, S. Turck-Chieze, J. B. Bellicard, M. Huet, P. Leconte, X.-H. Phan, I. Sick, J. Heisenberg, M. Girod, K. Kumar, B. Grammaticos, Physics Letters B, 122, 5 (1983) 347–350.
[13]R. B. M. Mooy and P. W. M. Glaudemans, Nuclear Physics A, 438 (1985) 461–481.
[14]P. K. Raina and S. K. Sharma, Phy. Rev. C, 37, 4 (1988) 1427.
[15]M. Honma, T. Otsuka, B. a. Brown, T. Mizusaki, Physical Review C - 69 (2004) 034335.
[16]O. V. Bespalova, I. N. Boboshin, V. V. Varlamov, T. a. Ermakova, B. S. Ishkhanov, a. a. Klimochkina, S. Y. Komarov, H. Koura, E. a. Romanovsky, T. I. Spasskaya, Bulletin of the Russian Academy of Sciences: Physics, 74, 4 (2010) 542.
[17]J. M. Allmond, B. a. Brown, a. E. Stuchbery, A. Galindo-Uribarri, E. Padilla-Rodal, D. C. Radford, J. C. Batchelder, M. E. Howard, J. F. Liang, B. Manning, R. L. Varner, C.-H. Yu, Physical Review C, 90 (2014) 1–6.
[18]J. M. Yao, M. Bender, P. H. Heenen, Phys. Rev. Lett. 113 (2014) 1–18
[19]R. A. Radhi, "A computer program to calculate, the elastic and inelastic electron scattering form factor for Coulomb electric and magnetic multipoles, including core – polarization effects.," (2009).
[20] J. C. Bergestrom, I. P. Auer, M. Ahmed, F. J. Kline, J. H. Hough, H.S. Caplan, J. L. Groh, Phys. Rev. C7, N6 (1973) 2228.
[21] R. A. Radhi, A. Bouchebak, Nucl. Phys., A716, (2003) 87.
[22] P. J. Brussard and P. W. M. Glademans, North-Holland Publishing Company, Amsterdam (1977).
[23]H. Nakada, Physical Review, C 78 (2008) 1–13.
[24]B. A. Brown, Phys. Rev, C, 58 (1998) 220.